Fish oil increases raft size and membrane order of B cells accompanied by differential effects on function[S]

Benjamin Drew Rockett,* Heather Teague,* Mitchel Harris,* Mark Melton,* Justin Williams,[†] Stephen R. Wassall,[†] and Saame Raza Shaikh[1,*]

Department of Biochemistry and Molecular Biology,* Brody School of Medicine, East Carolina Diabetes and Obesity Institute, East Carolina University, Greenville, NC 27834; Department of Physics,[†] Indiana University-Purdue University Indianapolis, Indianapolis, IN 46202

Abstract Fish oil (FO) targets lipid microdomain organization to suppress T-cell and macrophage function; however, little is known about this relationship with B cells, especially at the animal level. We previously established that a high FO dose diminished mouse B-cell lipid raft microdomain clustering induced by cross-linking GM1. To establish relevance, here we tested a FO dose modeling human intake on B-cell raft organization relative to a control. Biochemical analysis revealed more docosahexaenoic acid (DHA) incorporated into phosphatidylcholines than phosphatidylethanolamines of detergent-resistant membranes, consistent with supporting studies with model membranes. Subsequent imaging experiments demonstrated that FO increased raft size, GM1 expression, and membrane order upon cross-linking GM1 relative to no cross-linking. Comparative in vitro studies showed some biochemical differences from in vivo measurements but overall revealed that DHA, but not eicosapentaenoic acid (EPA), increased membrane order. Finally, we tested the hypothesis that disrupting rafts with FO would suppress B-cell responses ex vivo. FO enhanced LPS-induced B-cell activation but suppressed B-cell stimulation of transgenic naive CD4$^+$ T cells. Altogether, our studies with B cells support an emerging model that FO increases raft size and membrane order accompanied by functional changes; furthermore, the results highlight differences in EPA and DHA bioactivity. —Rockett, B. D., H. Teague, M. Harris, M. Melton, J. Williams, S. R. Wassall, and S. R. Shaikh. **Fish oil increases raft size and membrane order of B cells accompanied by differential effects on function. *J. Lipid Res.* 2012.** 53:**674–685.**

Supplementary key words antigen-presenting cell • cytokines • detergent resistant membrane • docosahexaenoic acid • lymphocytes.

Fish oil (FO) enriched in n-3 polyunsaturated fatty acids (PUFAs) is increasingly hypothesized to have beneficial health effects for treating symptoms for a wide range of diseases associated with chronic inflammation (1–3). However, several hurdles have prevented the therapeutic use of FO in the clinic, including a limited understanding of the molecular targets and mechanisms of n-3 PUFAs. The proposed mechanisms by which the n-3 PUFAs of FO, eicosapentaenoic acid (EPA) and docosahexaenoic acid (DHA), exert immunosuppressive effects are pleiotropic (4). These include incorporating into membrane phospholipids and modifying plasma membrane microdomain organization, serving as precursors for bioactive lipid molecules, disrupting intracellular signaling, and regulating gene expression (4). Recently, manipulation of lipid raft microdomains with n-3 PUFAs has gained attention because this mode of action is central to many of the downstream effects of n-3 PUFAs (5).

Several models, which are not in complete agreement, have emerged to explain how n-3 PUFAs disrupt raft molecular organization. One model, based on ex vivo studies of the CD4$^+$ T-cell immunological synapse, is that n-3 PUFAs, relative to controls, enhance the formation of more ordered and possibly larger lipid rafts upon stimulation of the cell (6). This model is the most relevant because it relied on the fat-1 transgenic mouse that has higher endogenous levels of n-3 PUFAs compared with control mice. A second model developed with studies in model membranes is that phosphatidylethanolamines containing DHA largely avoid raft molecules to form their own entities as nonraft domains (7, 8). Finally, a more integrated model, based mostly on in vitro studies, is that n-3 PUFAs incorporate directly into rafts and in some cell types force cholesterol molecules to undergo displacement between rafts and nonrafts (5, 9, 10). Overall, the majority of these models have not relied on physiologically relevant conditions that model human intake of FO.

The work was supported by National Institutes of Health Grant R15AT006122 (S.R.S.). Its contents are solely the responsibility of the authors and do not necessarily represent the official views of the National Institutes of Health. B.D. Rockett, H. Teague, M. Harris, M. Melton, J. Williams, S.R. Wassall, S.R. Shaikh, no conflicts of interest.

Manuscript received 21 October 2011 and in revised form 26 January 2012.

Published, JLR Papers in Press, February 7, 2012
DOI 10.1194/jlr.M021782

Abbreviations: CON, control diet; DHA, docosahexaenoic acid; DRM, detergent-resistant membrane; DSM, detergent-soluble membrane; EPA, eicosapentaenoic acid; FO, fish oil; GP, generalized polarization; OVA$_{323–339}$, chicken ovalbumin 323–339; PC, phosphatidylcholine; PE, phosphatidylethanolamine; TIRF, total internal reflection fluorescence.

[1]To whom correspondence should be addressed.
e-mail: shaikhsa@ecu.edu

[S]The online version of this article (available at http://www.jlr.org) contains supplementary data in the form of two tables and three figures.

Based on studies with $CD4^+$ T cells, macrophages, and splenocytes, disruption of rafts with n-3 PUFAs generally suppresses cellular function (6, 11, 12). Far less is known about the relationship between disruption of lipid rafts with n-3 PUFAs and downstream function in other cell types. In particular, B cells are increasingly recognized to have a role in inflammatory processes and autoimmune diseases (13, 14); however, there is limited understanding about how FO affects B-cell membrane organization and function, especially at the animal level. We previously demonstrated that feeding C57BL/6 mice a very high dose of n-3 PUFAs for 3 weeks diminished B-cell lipid raft clustering (15). We also showed that mice consuming this very high dose for 14 weeks displayed enhanced B-cell activation, which we speculated was due to an increase in body weight (16). However, we did not completely test the effects of a physiologically relevant dose of FO on raft organization, the mode of raft disruption, or its relationship with innate and adaptive B-cell function.

The specific objectives of this study were *1*) to determine if administration of a dose of FO, modeling human intake, disrupted lipid raft organization of mouse B cells; *2*) to address the conflicting models on how n-3 PUFAs disrupted raft molecular organization; and *3*) to test the hypothesis that altering raft organization with FO would promote immunosuppressive effects on downstream innate and adaptive B-cell function. The approach relied on biochemical and imaging measurements of B cells isolated from mice fed FO, supplemented with in vitro and model membrane studies. The data revealed for the first time that a relevant dose of FO increased B-cell raft size and membrane molecular order upon cross-linking rafts, which was accompanied by novel downstream functional effects.

MATERIALS AND METHODS

Mice and diets

Male C57BL/6 mice (Charles River), 4–6 weeks old, were fed for 3 weeks a purified control (CON) diet or a FO diet (Harlan-Teklad). Both diets consisted of 5% total fat by weight or 13% by total energy. All ingredients were essentially identical except the fat source, which was soybean oil in the CON diet and menhaden fish oil in the FO diet (**Table 1**). The FO diet also contained food coloring, which we ensured had no effects on the measurements described below. The fatty acid distribution of the diet, measured with GC, was within experimental error to that reported by the vendor (Harlan-Teklad) (Supplementary Table I). Approximately 2% of the total kcal came from EPA and 1.3% from DHA. This level of EPA/DHA corresponded to approximately 4 g of FO consumed by a human on a daily basis, which can be achieved through the diet and is currently in use pharmacologically for treating elevated triglycerides (17). Mice were euthanized using CO_2 inhalation and cervical dislocation followed by isolation of spleens. All of the experiments with mice fulfilled the guidelines established by the East Carolina University Brody School of Medicine for euthanasia and humane treatment.

TABLE 1. Composition of control and fish oil diets

Formula	Control	Fish oil
	g/Kg	
Casein	185.0	185.0
L-cystine	2.5	2.5
Corn starch	369.98	369.88
Maltodextrin	140.0	140.0
Sucrose	150.0	150.0
Cellulose	50.0	50.0
Soybean oil	50.0	—
Fish oil	—	50.0
Mineral mix, AIN-93M-MX (94049)	35.0	35.0
Vitamin mix, AIN-93-VX (94047)	15.0	15.0
Choline bitartrate	2.5	2.5
TBHQ, antioxidant	0.02	0.02
Yellow food coloring	—	0.1

Cell isolation and cell culture

$B220^+$ B cells (> 90% purity) were isolated from splenocytes by negative selection (Miltenyi Biotech) as previously described (16). For some experiments, $CD4^+$ T cells (> 85% purity) were purified from B6.Cg-Tg(TcraTcrb)425Cbn/J mice (OT-II) (Jackson Laboratory) that express α- and β-chain T-cell receptor and CD4 co-receptor specific for recognizing chicken ovalbumin 323–339 ($OVA_{323–339}$) presented by H-2 IAb molecules. For in vitro studies, mouse EL4 lymphomas were treated with 25 μM EPA or DHA complexed to BSA for 15.5 h as previously described (18). BSA without complexed fatty acid served as the control (18).

Isolation of detergent-resistant membranes and analysis

A total of 30×10^6 B cells or 20×10^6 EL4 cells were prepared for detergent extraction and layered on a sucrose gradient as previously described (18). Sucrose gradients were centrifuged at 40,000 rpm for 20 h at 4°C in a swinging bucket SW41Ti rotor (Beckman). Twelve 1 ml fractions were collected. Fractions 3–6 representing detergent-resistant membranes (DRMs) or fractions 9–12 representing detergent-soluble membranes (DSMs) were combined based on their cholesterol content, which was measured with an Amplex Red cholesterol assay kit (Invitrogen) relative to protein levels. Lipids were extracted as described previously (18). Samples were dissolved in chloroform, and select phospholipids were separated with a Shimadzu Prominence HPLC using a 150 × 4.6 mm Luna 5 μm NH_2 column (Phenomenex) with a mobile phase gradient of H_2O (increasing from 5% to 50%) and acetonitrile (decreasing from 95% to 50%) at 30°C. Phosphatidylethanolamine (PE), phosphatidylcholine (PC), and sphingomyelin (SM) fractions were collected by UV detection at 202 nm, and the acyl chain composition of each fraction was further analyzed by GC as previously shown (18). The rationale for selecting these phospholipids was to address the most abundant lipids of the outer (PC, SM) and inner (PE) leaflets and to allow direct comparison with other studies (19).

^2H NMR spectroscopy

Sample preparation, NMR spectroscopy, and analysis were as previously described (7). The PC phospholipid (1-[$^2H_{31}$] palmitoyl-2-docosahexaenoylphosphatidylcholine,16:0-22:2PC-d_{31}) used for this study was perdeuterated in the sn-1 chain (custom synthesis, Avanti Polar Lipids), and the samples consisted of aqueous multilamellar dispersions of 50 wt% lipid in 50 mM Tris buffer (pH 7.5). Briefly, lipid mixtures of 16:0-22:6PC-d_{31}/SM (1:1) and 16:0-22:6PC-d_{31}/SM/cholesterol (1:1:1) were codissolved in chloroform. The solvent was removed, the lipids were hydrated with buffer, and the pH was adjusted. After three lyophilizations with deuterium-depleted water (Sigma), samples were transferred to a 5 mm NMR tube. Stringent precautions were taken to prevent oxidation during sample preparation and data acquisition. NMR experiments were performed on a home-built spectrometer operating at 7.05 T using a phase-alternated quadrupolar echo sequence (8, 20).

Lipid raft cross-linking and total internal reflection fluorescence imaging

Cells were fluorescently stained for lipid rafts by cross-linking cholera toxin subunit B-FITC (CTxB) (Invitrogen) and then imaged using total internal reflection fluorescence (TIRF) microscopy. For select experiments, GM1 levels were measured by staining with primary with no secondary antibody for cross-linking. TIRF was performed on an Olympus IX-71 microscope with excitation at 488 nm by a 20 mW Sapphire laser and a 60× 1.45NA oil-immersion TIRF objective. Fluorescence emission was filtered through a LF-488/561-A-OMF filter cube (Semrock) and detected by a Hamamatsu ORCA-R2 progressive scan interline CCD camera. For all imaging experiments, 9 or 10 cells per diet were analyzed per experiment, and image analysis was performed as previously described (18).

Live cell imaging of $DiIC_{18}$

To assess changes in nonraft organization, we measured uptake of the nonraft probe 1,1′-dioctadecyl-3,3,3′,3′-tetramthylindocarbocyanine perchlorate ($DiIC_{18}$, Invitrogen) (21). The approach was similar to our previous report where we used FAST-DiI (15). However, FAST-DiI uptake was extremely rapid under live cell imaging conditions; therefore, we relied on $DiIC_{18}$. A total of 1×10^6 B cells were washed with RPMI 1640 without phenol red at 37°C and resuspended in 1 ml of the same media and placed into Delta T dishes (Bioptechs Inc.). We added 0.2 μl of a 1 mg/ml stock of $DiIC_{18}$ to the dishes and imaged. Live cell, wide-field microscopy was conducted with an Olympus IX-70 microscope using an oil 100× objective and a Hamamatsu CCD camera, equipped with stage and objective heaters (Bioptechs Inc.). Imaging was started at 1 min after addition of the fluorescent probe at 37°C. Images were acquired with MetaMorph software and analyzed with NIH ImageJ. All settings were kept constant between experiments.

Generalized polarization imaging

Generalized polarization (GP) was calculated to determine the molecular order of the B and EL4 cell plasma membrane (22). Cells were stained with 4 μM di-4-ANEPPDHQ (Invitrogen) for 30 min at 37°C, washed twice with PBS, and fixed with 4% paraformaldehyde (23). For some experiments, as an additional control, B cells were treated with 10 μM methyl-β-cyclodextrin (Sigma-Aldrich) for 15 min at 37°C to deplete cholesterol. Imaging was conducted on a Zeiss LSM-510 confocal microscope using a 100× objective with excitation at 488 nm and fluorescence emission detected in two channels: 505–545 nm for ordered regions and 650–750 nm for disordered regions. Quantification of fluorescence intensity (I), after background subtraction for the two channels, was performed using NIH ImageJ. GP was calculated using the formula: $GP = (I_{505–545} - (G)I_{650–750})/(I_{505–545} + (G)I_{650–750})$, where G is the G-factor and I is fluorescence intensity (22).

B-cell activation with LPS

B cells were stimulated with 1 μg/ml of LPS for 24 h, and the secreted cytokine profiles were measured from supernatants using a Multi-Analyte ELISArray kit (SA Biosciences) as previously demonstrated (16). In addition, B cells were analyzed for surface expression of activation markers using fluorescently labeled anti-major histocompatibility complex II (MHC class II) M5/114.15 (Bio X Cell), anti-CD69 H1.2F3 (BD Biosciences), and anti-CD80 16-10A1 (Bio X Cell) on a BD LSR II flow cytometer. Antibodies for MHC class II and CD80 were conjugated with fluorophores using a kit (GE Healthcare).

B-cell activation of naive $CD4^+$ T cells

B cells were peptide loaded with $OVA_{323–339}$ (GenScript) at various concentrations in serum-free media for 1 h at 37°C and then washed with fresh media. A total of 1×10^5 B cells were then plated with 3×10^5 nondiet modified OT-II transgenic T cells, spun quickly, and incubated for 24 h at 37°C in 96-well plates. After 24 h, the supernatant was collected to analyze secreted IFN-γ and IL-2 with an ELISArray kit (SA Biosciences) following the manufacturer's protocol. The cells were stained with fluorescently labeled anti-CD4-PE (Miltenyi Biotech), anti-CD69-FITC (BD Biosciences), and anti-CD25-PE-Cy7 (BD Biosciences) and analyzed by flow cytometry on a BD LSR II. In all flow cytometry experiments, SYTOX Blue (Invitrogen) was used to discriminate dead cells, and at least 10,000 live events were collected for analyses. Control experiments were routinely conducted in the absence of peptide and with T cells only (no B cells) to ensure T-cell activation was driven by peptide-loaded B cells.

Statistical analyses

All ex vivo and in vitro data are from several independent experiments, with each ex vivo experiment representing one mouse per diet. The only exception was the ex vivo DRM/DSM analysis, in which two mice were pooled per experiment. Data were first analyzed for normality using a Kolmogorov-Smirnov test (GraphPad Prism). For a few select experiments with nonparametric distributions, we relied on paired Wilcoxon *t*-tests. Pairing was required due to differences in experimental settings between experiments as previously described (15). For the majority of animal experiments, statistical significance was established using an unpaired one-tailed or two-tailed Student's *t*-test. One-tailed unpaired *t*-tests were used to analyze the GC data from animals because before experimentation we predicted an increase in n-3 PUFA levels (19). In vitro studies relied on one-way ANOVAs followed by a Dunnett's post hoc *t*-test (16). *P* values less than 0.05 were considered significant. The NMR data were not analyzed for statistical significance because they were obtained on model membranes of well defined and controlled composition for which a reproducibility of ±1% applies to multiple acquisitions. This approach is standard for model membrane studies using NMR spectroscopy (7, 8).

RESULTS

Body weights, food intake, and cellularity

The FO diet, relative to CON, had no effect on the rate of body weight gain (Supplementary Fig. IA) or food intake per day (Supplementary Fig. IB). Spleen weight (Supplementary Fig. IC) was significantly elevated for mice on the FO diet but did not affect the steady-state number of B cells (data not shown). Given that we recently reported n-3 PUFAs at high doses can lower energy expenditure (24), we verified that the FO diet had no impact on whole body energy expenditure using metabolic cages (data not shown).

FO promoted uptake of EPA/DHA into DSMs and DHA into PC of DRMs

The first objective was to biochemically determine if the physiologically relevant dose of FO manipulated the molecular composition of B-cell "raft"-like DRMs. We used detergent extraction followed by HPLC-GC to determine the acyl chain composition of PE, PC, and SM ex vivo (**Fig. 1**). The relative proportion of PC, PE, and SM in DRM and DSM fractions was not changed by FO (Fig. 1A). Relative PC and SM levels were generally higher in DRMs than in DSMs. SM was the smallest fraction of PE/PC/SM, consistent with studies in other cell types (25).

In PE, EPA (20:5) and DHA (22:6) did not incorporate into DRMs but were significantly increased in DSMs (Fig. 1B). FO also increased 22:5 and lowered arachidonic acid (20:4) in PE DSMs (Fig. 1B). In PC, 20:5 was lowered and 22:6 increased with FO in DRMs ($P = 0.06$) (Fig. 1C). In DSMs of PC, 20:5 and 22:6 did not significantly increase (Fig. 1C). In SM, 20:5 and 22:6 did not change in DRMs (Fig. 1D). In DSMs of SM, FO significantly decreased palmitic acid (16:0) and increased stearic acid (18:0), 20:5, 22:5, and 22:6 (Fig. 1D). Because we did not quantify the exact levels of EPA and DHA, we conducted a few select experiments to approximate the levels EPA and DHA incorporating into DRMs and DSMs (data not shown). On average, ~5–8% of the total n-3 PUFA were localized to

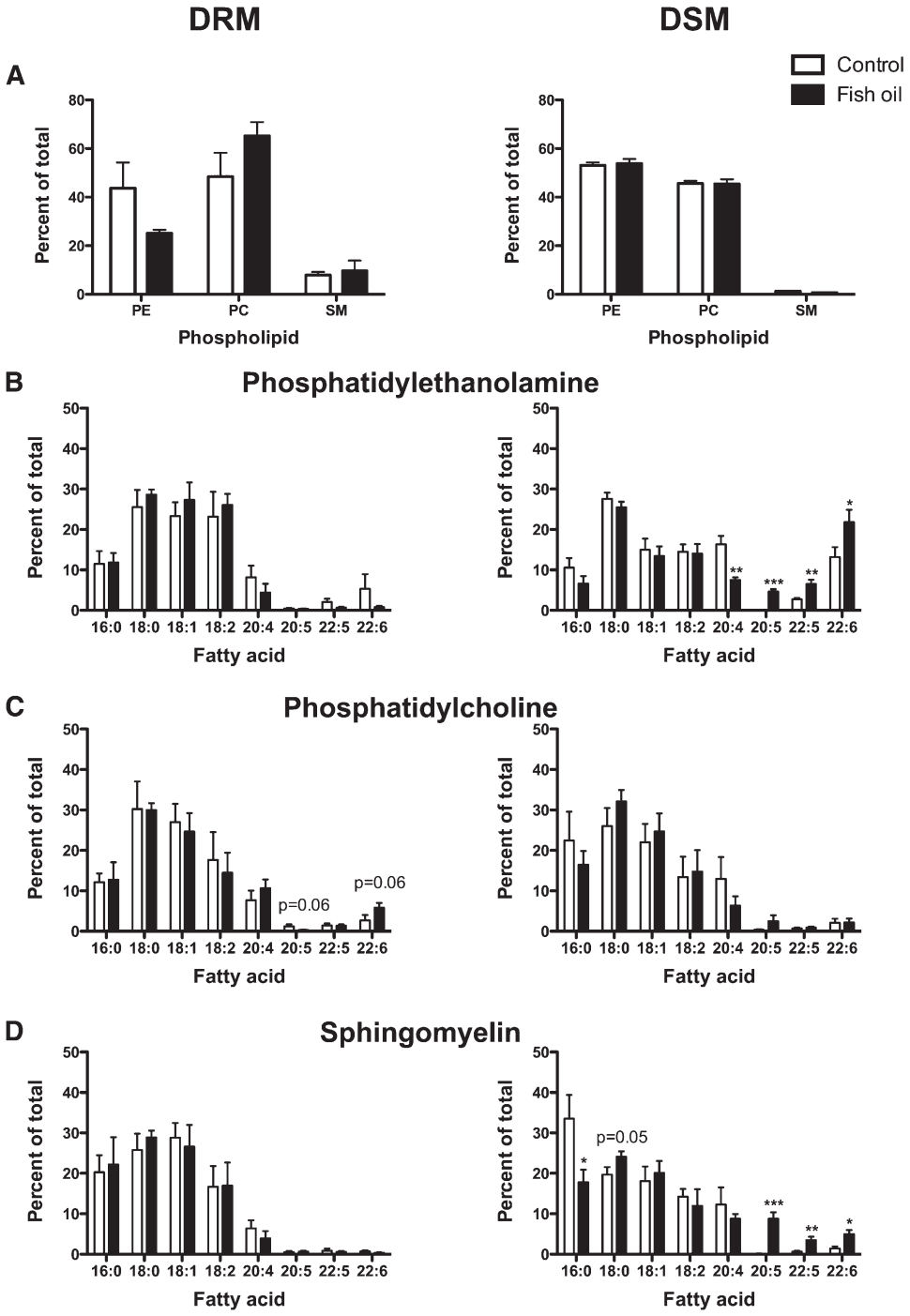

Fig. 1. FO promoted uptake of EPA/DHA into DSMs and DHA into PC of DRMs. A: Relative levels of B-cell PE, PC, and SM of DRM (left) and DSM (right) fractions. Acyl chain composition of B-cell DRM or DSM fractions of (B) PE, (C) PC, and (D) SM. B cells were isolated from mice fed control or FO-enriched diets. Data are means ± SEM (n = 4, with two mice pooled per experiment). Asterisks indicate different from control: $*P < 0.05$; $**P < 0.01$; $***P < 0.001$.

DRMs with the remaining amount in DSMs, consistent with another study (26).

Cholesterol levels in DRM and DSM fractions were not changed with FO (Supplementary Table II). We also analyzed the ratio of DRM to DSM cholesterol based on a very recent study that reported that DHA treatment in vitro increased cholesterol into DSMs when analyzed as a ratio (9). FO had no effect on the ratio (Supplementary Table II).

Overall, the data were highly consistent with predictions from detergent-free model membrane studies in which PCs containing DHA were found to have higher solubility for cholesterol, and by implication to have more favorable interactions with rafts, than PEs containing DHA (27). We confirmed this by comparing the order of cholesterol on the perdeuterated sn-1 chain on a DHA-containing PC (16:0-22:6PC-d_{31}) vs. a DHA-containing PE (16:0-22:2PE-d_{31}) in mixtures with SM (1:1) and SM/cholesterol (1:1:1), mimicking rafts, using ^{2}H NMR spectroscopy (**Table 2**). The increase in order due to cholesterol (reflecting proximity), measured for the PC-containing DHA, was more than twice that for the PE-containing DHA (Table 2). This observation was consistent with the ex vivo biochemical data that suggest DHA infiltrated into PCs of DRMs and PEs of DSMs.

TABLE 2. DHA-containing PC displayed increased molecular order in the presence of lipid raft molecules relative to PE

Lipid Mixture	Order Parameter Value	Percent Increase in Order
16:0-22:6PC-d_{31}/sphingomyelin	0.115	68.7%
16:0-22:6PC-d_{31}/sphingomyelin/cholesterol	0.194	
16:0-22:6PE-d_{31}/sphingomyelin	0.150	26.0%
16:0-22:6PE-d_{31}/sphingomyelin/cholesterol	0.189	

Average order parameter values were calculated from ^{2}H NMR spectra collected at 40°C for mixtures of 16:0-22:6PC-d_{31} with sphingomyelin (1:1) and with sphingomyelin and cholesterol (1:1:1). Values for 16:0-22:6PE-d_{31} were from previously published data (7).

FO increased B-cell lipid raft size induced by cross-linking GM1

The next objective was to measure changes in raft organization with the FO diet relative to the CON diet using microscopy. This was essential because biochemical approaches are a useful predictive tool but also have limitations due to the use of detergent (28, 29). TIRF imaging of B cells from FO- and CON-fed mice showed a significant difference in the spatial distribution of GM1 molecules cross-linked with CTxB (**Fig. 2A**). TIRF image analysis, confirmed with confocal image analysis (data not shown), revealed the Feret's diameter was increased by 79% with FO relative to CON (Fig. 2B). The binding of CTxB to GM1 in the presence of cross-linking, measured in terms of fluorescence intensity, showed on average a 36% increase with FO, but this failed to reach statistical significance with TIRF analysis (Fig. 2C). To determine if the propensity for an increase in CTxB intensity was due to increased surface levels of GM1, the binding of CTxB in the absence of cross-linking was measured, which revealed a 49% increase in intensity with FO (Fig. 2D). To ensure the observed effects were FO specific, we also measured raft size and binding of CTxB with a safflower oil-enriched diet and found no evidence of raft disruption with this diet (Supplementary Fig. II). We also ensured the effects were specific for rafts. Changes in nonraft organization were measured in terms

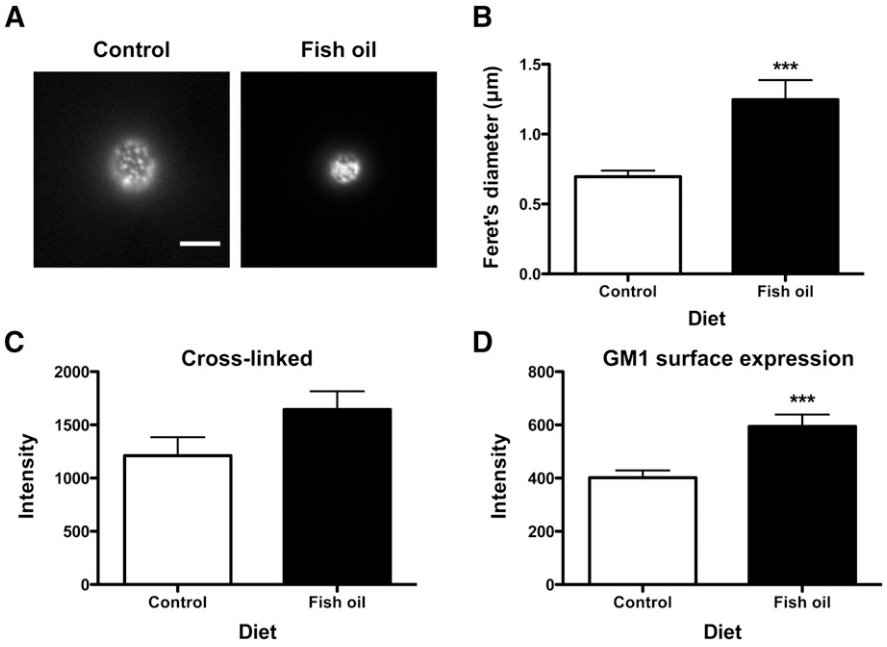

Fig. 2. FO increased the size of rafts induced by CTxB cross-linking. A: Sample fluorescence images of B cells isolated from control or FO-fed mice and cross-linked to induce raft clustering. Images are from TIRF microscopy (bar, 5 μm). B: Lipid raft size in terms of Feret's diameter for B cells. C: CTxB fluorescence intensity after cross-linking. D: GM1 surface levels. Values are means ± SEM (n = 6 for A–C; n = 4 for D). Asterisks indicate different from control: ***$P < 0.001$.

of uptake of the nonraft probe $DiIC_{18}$ (21). Live cell imaging revealed that $DiIC_{18}$ uptake was identical between cells isolated from CON- and FO-fed mice (Supplementary Fig. III). The imaging results provided the first evidence that a physiologically relevant dose of FO disrupted raft, but not nonraft, organization.

FO increased membrane order upon cross-linking rafts relative to the absence of cross-linking

We subsequently determined if the aforementioned changes with FO on raft organization affected membrane molecular order. This directly addressed two opposing models in which n-3 PUFAs in response to stimulation increase membrane order ex vivo versus a decrease in membrane order in vitro (6, 25). To measure molecular order, we used di-4-ANEPPDHQ, an environmental sensing fluorescent dye that can shift its emission spectra 30 nm depending on the degree of packing in the surrounding lipid chains (**Fig. 3A**) (30). As an initial control, B cells were treated with 10 μM methyl-β-cyclodextrin to remove cholesterol from the membrane. GP significantly decreased upon cholesterol depletion (data not shown). In the absence of cross-linking, FO, compared with CON, significantly decreased the average GP by 25% (Fig. 3B). This decrease was consistent with data showing that n-3 PUFAs exert a disordering effect on membrane microviscosity in the absence of inducing raft formation (31). Although there was no difference in GP values between CON and FO diets upon cross-linking (Fig. 3C), GP values for FO were elevated to a greater extent than CON relative to no cross-linking (Fig. 3D). Analysis of the differences in GP values between cross-linking and no cross-linking showed FO had a greater ordering effect by 65% compared with CON (Fig. 3D). These results supported the ex vivo model that FO is capable of exerting an ordering effect on the membrane upon stimulation (6).

EPA and DHA incorporated into DRMs/DSMs and did not increase GM1 surface expression in vitro

We previously reported that treatment of EL4 cells with DHA, but not EPA, increased raft size (18). Therefore, we conducted comparative biochemical and imaging studies to determine if the in vivo and in vitro modes of raft disruption were similar in addition to discriminating differences in bioactivity of EPA vs. DHA.

Similar to ex vivo measurements, relative PC and SM levels were higher in DRMs than in DSMs and were not affected by EPA or DHA (**Fig. 4A**). In PE, EPA treatment increased 20:5 and 22:5 in DRMs. DHA treatment had no significant effect on 22:6 in DRMs of PE (Fig. 4B). In PE DSMs, EPA and DHA treatment lowered 20:4 and DHA increased 22:6 (Fig. 4B). In PCs, EPA and DHA treatment did not significantly increase 20:5 or 22:6 in DRMs (Fig. 4C). In PC DSMs, EPA and DHA treatment, respectively, increased 20:5/22:5 and 22:6 levels. EPA and DHA treatment lowered 18:1 in DRMs and DSMs of PC. In SM, EPA and DHA, respectively, increased 20:5 and 22:6 in DRMs (Fig. 4D). In DSMs of SM, EPA and DHA lowered 18:1 and, respectively, increased 20:5/22:5 and 22:6. Similar to the ex vivo studies, we did not quantify exact levels of EPA and DHA in DRM/DSM. Based on a few select studies (data not shown), ~30% of the

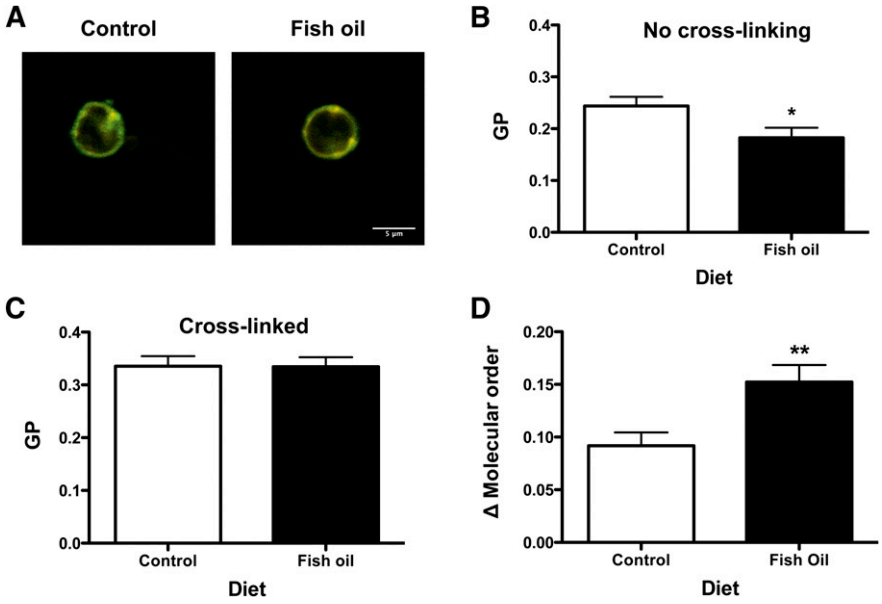

Fig. 3. FO increased B-cell membrane molecular order upon cross-linking relative to no cross-linking. A: Sample merged intensity images of B cells, stained with di-4-ANEPPDHQ, isolated from control or FO-enriched diets. Ordered (green) and disordered (red) channels are merged to illustrate the ratio between channels. B: Plasma membrane GP values from B cells isolated from control and FO-fed mice without CTxB cross-linking. C: GP analysis of B cells cross-linked with CTxB. D: Change in GP values upon cross-linking CTxB relative to no cross-linking. Values are means ± SEM (n = 4). Asterisks indicate different from control: $*P < 0.05$; $**P < 0.01$.

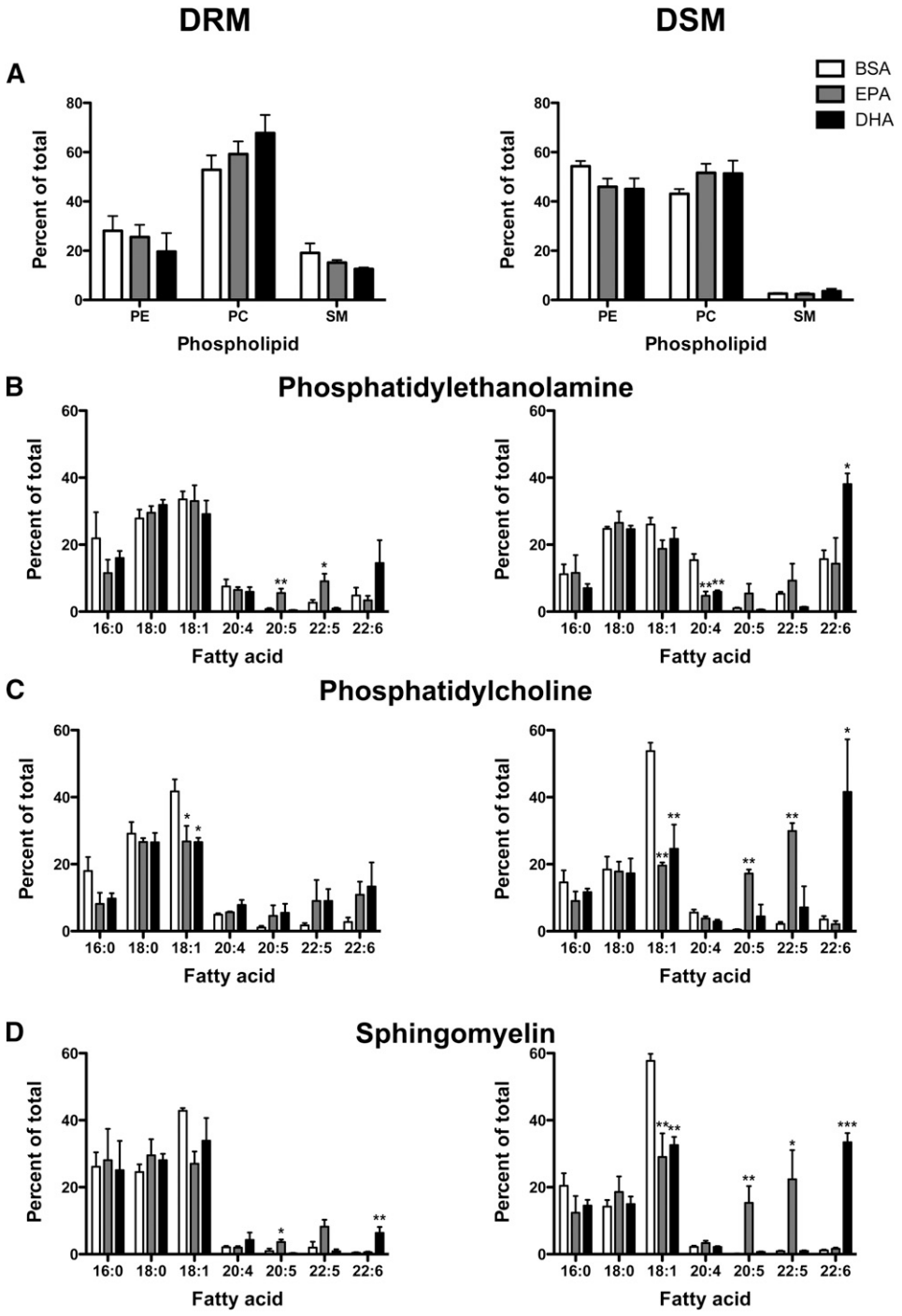

Fig. 4. EPA and DHA treatment targeted DRM and DSM composition of EL4 cells. A: Relative levels of PE, PC, and SM of EL4 DRM (left) and DSM (right) fractions. Acyl chain composition of DRM or DSM fractions from (B) PE, (C) PC, and (D) SM. EL4 cells were treated with BSA, 25 μM EPA, or DHA. Values are means ± SEM (n = 4). Asterisks indicate different from control: $*P < 0.05$; $**P < 0.01$; $***P < 0.001$.

added EPA/DHA was localized to DRMs with the remaining amount in DSMs, consistent with our previous work (18).

Cholesterol levels in the DRM and DSM fractions were not significantly changed with EPA or DHA treatment (Supplementary Table II). There was a tendency for EPA treatment to lower DRM cholesterol relative to BSA when analyzed as a *t*-test ($P < 0.05$). The ratio of cholesterol in DRM to DSM also had a tendency to be lowered with EPA and DHA treatment ($P = 0.08$) (Supplementary Table II). Finally, we measured GM1 surface levels using microscopy before and after cross-linking and found no effect of EPA or DHA treatment (Supplementary Fig. IV). These results showed that in vitro treatment with EPA/DHA, consistent with most other in vitro studies, changed DRM composition (19, 32); however, we did not measure an increase in GM1 levels in vitro with EPA or DHA treatment as observed ex vivo.

DHA, but not EPA, increased membrane order with cross-linking relative to the absence of cross-linking in vitro

We next determined if EPA and DHA treatment increased membrane order as measured ex vivo. In the absence of cross-linking, EPA and DHA, respectively, compared with BSA, decreased GP by 32% and 75% (**Fig. 5A**). Upon cross-linking, EPA showed no difference in molecular order relative to BSA; however, DHA treatment lowered GP by 27% (Fig. 5B). Analysis of the differences in GP values between cross-linking relative to no cross-linking showed DHA, but not EPA, had a greater ordering effect by 60% compared with BSA (Fig. 5C). These results supported the emerging ex vivo model that an n-3 PUFA exerts an ordering effect upon induction of raft formation (6).

FO enhanced B-cell activation in response to LPS stimulation but suppressed B-cell stimulation of naive CD4$^+$ T cells

The next set of experiments tested the hypothesis that disruption of lipid raft organization with FO would be accompanied by suppressive effects on downstream innate and adaptive B-cell function, as reported for T cells, macrophages, and splenocytes (6, 11, 12). Two different B-cell functional studies were conducted. First, we measured the activation of B cells after 24 h of LPS stimulation as a measure of an innate response (**Fig. 6**). We found the physiologically relevant dose of FO enhanced B-cell activation. The number of B cells activated was the same between the CON and FO diets (data not shown). CD69 surface levels were increased by 22% with FO, whereas MHC class II and CD80 surface expression were not affected by FO (Fig. 6A). Secretion of IL-6, TNF-α, and IFN-γ were increased compared with FO relative to the CON by 43, 87, and 182% (Fig. 6B). IL-10 secretion was unaffected with the FO diet (Fig. 6B).

To determined if the immune enhancing effect of the FO diet on B cells was specific to the innate response or applicable to an adaptive immune response, we tested the ability of B cells isolated from FO-fed mice to stimulate transgenic naive CD4$^+$ T cells that were not from FO-fed mice (**Fig. 7**). The concentration of $OVA_{323–339}$ peptide loaded into B cells was optimized for maximal activation at 10^{-5} M with no activation at 0 M (data not shown). FO had no impact on the percentage of CD4$^+$CD69$^+$CD25$^+$ T cells activated (data not shown). In addition, the surface expression of the activation markers CD69 and CD25 on CD4$^+$ T cells was unchanged with FO (Fig. 7A). Analysis of secreted cytokines revealed that IFN-γ levels were not significantly decreased with FO, but IL-2 secretion was decreased by 42% with the FO diet relative to CON (Fig. 7B). These results supported the notion that raft disruption with FO was accompanied by changes in B-cell function.

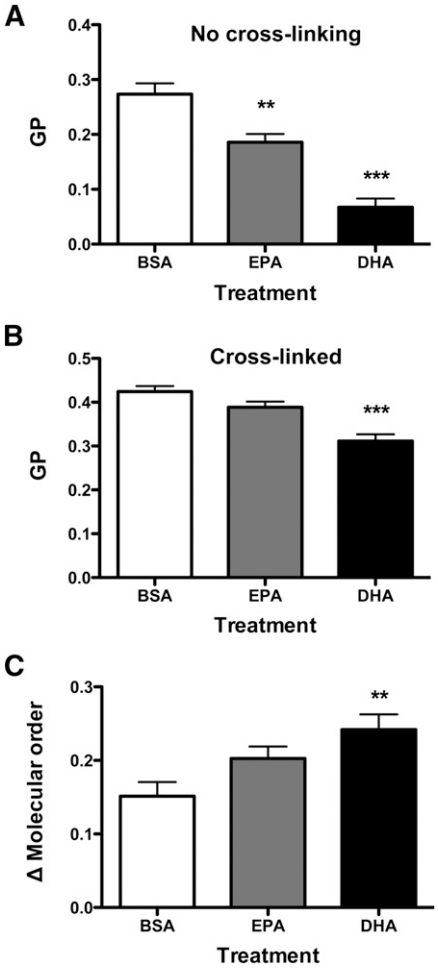

Fig. 5. DHA, but not EPA, increased membrane molecular order upon cross-linking relative to no cross-linking in vitro. A: Plasma membrane GP values from EL4 cells treated with BSA, EPA, or DHA without CTxB cross-linking. B: GP analysis of EL4 cells cross-linked with CTxB. C: Change in GP values upon cross-linking CTxB relative to no cross-linking. Values are means ± SEM (n = 3). Asterisks indicate different from control: $^{**}P < 0.01$; $^{***}P < 0.001$.

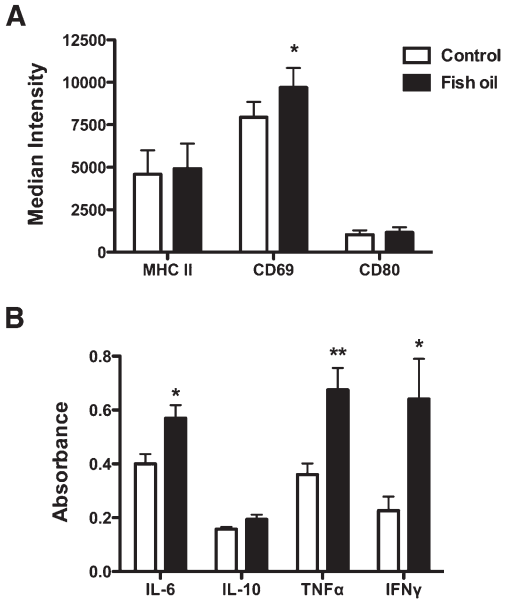

Fig. 6. FO increased B-cell CD69 expression and cytokine secretion upon activation with LPS. A: Median fluorescence intensity for B cells stained with anti-MHC class II, anti-CD80, or anti-CD69 after 24 h of LPS activation. B cells were isolated from mice fed a control or FO diet. B: Cytokine secretion after 24 h of LPS activation. Values are means ± SEM (n = 6). Asterisks indicate different from control: $^{*}P < 0.05$; $^{**}P < 0.01$.

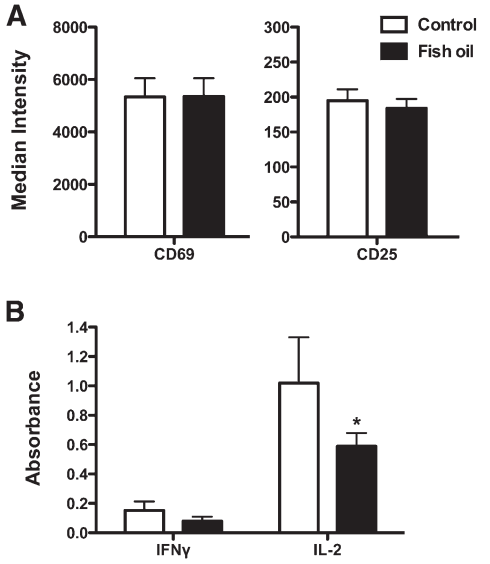

Fig. 7. FO suppressed B-cell stimulated IL-2 secretion from naive $CD4^+$ T cells. A: Median fluorescence intensity of $CD4^+$ T cells stained with anti-CD69 and anti-CD25 after 24 h. $CD4^+$ T cells were stimulated with B cells isolated from mice fed a control or FO diet. B: Cytokine secretion after 24 h of activation. Values are means ± SEM (n = 6). Asterisk indicates different from control: $*P < 0.05$.

DISCUSSION

In this study, we focused on B cells, a cell type underrepresented in experiments with n-3 PUFAs, especially at the animal level. The results demonstrated several significant advancements. First, the data showed that a relevant dose of FO increased the size of B-cell rafts. Next, data integrated from animals, cell culture, and model membranes challenged some models on how n-3 PUFAs disrupted raft molecular organization. Third, the data highlighted differences between EPA and DHA on membrane organization. Finally, we discovered that a physiologically relevant dose of FO enhanced an innate immune response but suppressed an adaptive response. Therefore, the data also challenged the paradigm that modification of rafts with FO exerts global immunosuppressive effects but overall supported the notion that manipulation of immune cell rafts with FO was accompanied by changes in function.

Biochemical measurements revealed some differences between ex vivo and in vitro measurements

The biochemical data from B cells (Fig. 1) were generally in agreement with ex vivo studies, with a few exceptions (12, 33). Fan et al. (34) demonstrated biochemically that n-3 PUFAs infiltrated DRMs and DSMs differentially depending on the type of headgroup. Their data showed the majority of n-3 PUFAs displayed a preference for inner leaflet lipids such as PEs. We also found greater incorporation of n-3 PUFAs into PEs over PCs. However, Fan et al. (34) reported that n-3 PUFAs incorporated in PE DRMs, whereas we observed the majority of n-3 PUFAs in DSMs of PEs (Fig. 1). We also found DHA in PC DRMs, whereas they found no n-3 PUFAs in PC DRMs. Finally, we observed an increase in surface levels of GM1, a sphingolipid, whereas the same group reported a decrease in SM in a subsequent study (33). The differences between the studies could be cell specific or due to differences in diet compositions.

The B-cell biochemical data showing DHA incorporated more into DRM PC than PE were consistent with model membrane experiments on lipid mixtures containing raft molecules (SM and cholesterol). They showed a DHA-containing PC underwent a greater increase in molecular order upon adding cholesterol compared with a DHA-containing PE (Table 2). These results were in agreement with previous studies to show cholesterol was more soluble in n-3 PUFAs containing PCs than PEs (27). It is also important to note that the DHA-containing PC underwent a substantial increase in molecular order when exposed to cholesterol in the mixture with SM, which was consistent with the increase in membrane molecular order observed ex vivo when comparing cross-linked rafts with the absence of cross-linking with FO (Fig. 3). Although n-3 PUFA acyl chains are highly disordered, very recent data from Mihailescu et al. (35) revealed that cholesterol could raise the order of a PC-containing DHA. Thus, the model membrane data suggest that a PC-containing DHA undergoing an ordering effect upon interaction with cholesterol would allow the PC-containing DHA to favorably incorporate into rafts.

Our ex vivo and in vitro data did not concur with some in vitro measurements from other labs on cholesterol lateral distribution in DRMs and DSMs. Grimm et al. (9) reported that treatment of SH-SY5Y cells with 100 μM DHA increased the normalized DSM/DRM ratio. We did not observe differences in cholesterol levels between DRM and DSMs in B cells or EL4 cells; however, the DRM/DSM ratio tended to be lowered in EL4 cells (Supplementary Table II). More work is clearly needed in this area because a very recent study reported that treatment of hepatocytes with EPA increased raft cholesterol levels, opposite of the findings reported by Grimm and coworkers (10).

There were a few differences between the B-cell biochemical data compared with the in vitro studies using EL4 cells. The first major difference was that GM1 levels were increased ex vivo with FO but not in vitro. The second major difference was that EPA/DHA did not dramatically infiltrate DRMs ex vivo compared with in vitro. Our in vitro data were in agreement with cell culture studies from other labs (19, 32). For example, Stulnig and coworkers showed that treatment of Jurkat T cells with EPA resulted in significant incorporation into DRMs and DSMs of SM, PC, and PEs (19). We also observed some uptake of n-3 PUFAs into the SM fraction in both cell types, similar to Stulnig's lab; however, it is possible that the SM fraction could contain some small contaminants from other phospholipids, such as phosphatidylinositols and phosphatidylserines.

Overall, we hypothesize that the differences between our ex vivo and in vitro studies were due to differences in cell type (primary vs. immortal) and methods of lipid delivery (diet vs. exogenous addition of EPA or DHA). Furthermore, the levels of fatty acids (data not shown) and cholesterol (Supplementary Table II) in EL4 cells were much higher than B cells, which was not surprising because EL4 cells are dramatically larger than primary B cells. Based on a few

select experiments, we observed that ~30% of the total n-3 PUFAs incorporated into DRMs of EL4 cells, whereas ~5–8% of the total n-3 PUFAs were in DRMs of primary B cells, generally consistent with previous work from our lab and others (18, 26). The significant incorporation of EPA/DHA into DRMs in EL4 cells was not due to the dose of fatty acid in culture because even low levels of EPA or DHA (5–20 μM) showed the same distribution within error into DRMs and DSMs (data not shown).

Imaging demonstrated that FO increased membrane order upon cross-linking

Detergent extraction is a predictive tool but can induce artifacts (28, 29). An alternative method would have been to conduct studies with detergent-free methods to isolate rafts (36); however, this was beyond the scope of the study. We discovered, consistent with other studies, that detergent-free methods required a very large number of cells ($>100 \times 10^6$) to isolate rafts (37). Therefore, we relied heavily on imaging to determine how FO disrupted raft organization upon CTxB cross-linking.

The ex vivo imaging data (Fig. 2, 3) were highly consistent with ex vivo data to show that fat-1 mice, which express high endogenous levels of n-3 PUFAs, displayed increased molecular order within the $CD4^+$ T-cell immunological synapse upon activation with a cognate hybridoma cell relative to nonsynapse regions (6). Similarly, we observed that cross-linking GM1 molecules of B cells from FO-fed mice had a greater increase in molecular order relative to no cross-linking (Fig. 3). Supporting in vitro studies showed DHA, but not EPA, increased membrane molecular order upon cross-linking relative to no cross-linking (Fig. 5). These results were novel because very little is known about the differences in bioactivity between EPA and DHA on membrane organization.

The ex vivo and in vitro imaging data were in agreement with our previous studies. We showed previously that treatment of EL4 cells with DHA, but not EPA, diminished CTxB-induced clustering of EL4 cells (18). We also discovered administration of a very high dose of a fish/flaxseed oil-enriched diet to mice disrupted B-cell raft organization with no impact on nonraft organization (15). The data in this study provide the first evidence for changes in B-cell raft organization with a physiologically relevant dose of FO.

Emerging model by which FO increases raft size

We propose the following working model to explain the ex vivo and in vitro data. In the absence of cross-linking, n-3 PUFA incorporation into the membrane, either through the diet or in culture, decreased membrane order due to the highly disordered nature of the n-3 PUFA acyl chains (31). In vivo, FO also enhanced GM1 surface levels, which could be due to targeting of GM1 biosynthesis and/or trafficking to the plasma membrane. Although the GM1 molecules were poised to form rafts in the absence of cross-linking, they were not in a state where large-scale phase separation could be observed (38, 39).

Upon cross-linking CTxB, the membrane became more ordered as lipid molecules were forced together and micron-scale domains became visible with FO. We speculate that FO administration resulted in the trapping of n-3 PUFAs into the large-scale raft domains. Cholesterol was not displaced out of the rafts in either model system. Instead, the mixing of cholesterol with n-3 PUFAs had an ordering effect on the membrane, as demonstrated with model membrane studies. In vitro studies demonstrated that the effects on membrane order were driven by DHA rather than by EPA. Overall, our data supported the model that FO can exert an ordering effect as opposed to the other models discussed above (6).

Disruption of rafts with FO was accompanied by differential effects on innate and adaptive B-cell functions

The previous work on how FO disrupts rafts and the subsequent impact on immune cell function has centered on $CD4^+$ T cells, macrophages, and splenocytes (6, 11, 12). Generally, manipulation of lipid microdomain organization (which may have utility as a biomarker of n-3 PUFA manipulation) with n-3 PUFAs was reported to be accompanied by immunosuppression. Here we discovered that LPS stimulation of B cells increased cytokine secretion (Fig. 6). The data were similar to a few studies showing that activation of splenic macrophages with LPS resulted in increased cytokine secretion with FO (40–42). The data were also in agreement with our previous report showing that very long-term administration of a high–fat, fish/flaxseed oil-enriched diet enhanced activation of B cells (16). We had previously suggested that the increase in B-cell activation was due to body weight gain, which we now know is not the driving factor.

The functional data (Fig. 6) were not entirely in agreement with some in vitro studies showing that DHA suppressed LPS activation of macrophages and dendritic cells (43–45). This could be due to aforementioned differences (e.g., cell type, diet vs. in vitro treatment, etc.). Increased proinflammatory cytokine secretion does not allow us to conclude that FO is proinflammatory. It is possible that increased B-cell activation could have potential clinical utility, especially in terms of antibody production. A few labs have studied the impact of FO on antibody production with mixed results (46–49). Altogether, these data highlighted the notion that FO is not universally immunosuppressive.

The antigen presentation data were the first to demonstrate that dietary manipulation of B cells with FO suppressed naive T-cell activation (Fig. 7). Our data confirmed several in vitro studies that showed EPA and/or DHA treatment of B cells, dendritic cells, and monocytes/macrophages diminished antigen presentation to cognate T cells (50, 51). The data were also consistent with one ex vivo study demonstrating a mixture of antigen-presenting cells (B cells, macrophages, DCs) isolated from a DHA-enriched diet suppressed the proliferation of naive $CD4^+$ T cells from mice fed control diets (52).

The functional data open the door to a wide range of new targets and mechanisms by which FO differentially affects B-cell function. The mechanisms downstream of the plasma membrane by which n-3 PUFAs enhance B-cell activation will require studying complex signaling pathways and their impact on gene activation. In the case of the antigen presentation studies, we now for the first time raise the possibility that lipid manipulation of the B-cell side of the immunological

synapse may be a major contributing factor by which T-cell activation was suppressed with n-3 PUFAs. It will be interesting to determine how manipulation of lipid microdomains can lead to an immune-enhancing effect with LPS and to a suppression of function when interacting with a T cell. It was beyond the scope of this study to address this, but it is something we aim to pursue in order to develop FO as a therapeutic agent for chronic inflammation.

CONCLUSION

We demonstrated that a physiologically relevant dose of FO increased the size of B-cell rafts, GM1 surface expression, and membrane molecular order upon cross-linking CTxB. Supporting in vitro studies suggested that the effects on membrane order were driven by DHA but not EPA. Furthermore, the B-cell data supported an emerging model that increasing raft size with FO was accompanied by changes in innate and adaptive function. Overall, the results established the utility of using a relevant dose of FO for the first time to target B-cell microdomain clustering and cellular function.

The authors thank Dr. Xiangming Fang for assistance with statistical analyses, Dr. Bill Stillwell and Dr. Robb Chapkin for useful discussions regarding interpretation of the data, and Dr. Richard Bazinet for assistance in discussing the HPLC-GC data.

REFERENCES

1. Calder, P. C. 2006. n-3 polyunsaturated fatty acids, inflammation, and inflammatory diseases. *Am. J. Clin. Nutr.* **83:** 1505S–1519S.
2. Duda, M. K., K. M. O'Shea, A. Tintinu, W. Xu, R. J. Khairallah, B. R. Barrows, D. J. Chess, A. M. Azimzadeh, W. S. Harris, V. G. Sharov, et al. 2009. Fish oil, but not flaxseed oil, decreases inflammation and prevents pressure overload-induced cardiac dysfunction. *Cardiovasc. Res.* **81:** 319–327.
3. Harris, W. S., D. Mozaffarian, M. Lefevre, C. D. Toner, J. Colombo, S. C. Cunnane, J. M. Holden, D. M. Klurfeld, M. C. Morris, and J. Whelan. 2009. Towards establishing dietary reference intakes for eicosapentaenoic and docosahexaenoic acids. *J. Nutr.* **139:** 804S–819S.
4. Calder, P. C. 2008. The relationship between the fatty acid composition of immune cells and their function. *Prostaglandins Leukot. Essent. Fatty Acids.* **79:** 101–108.
5. Yaqoob, P., and S. R. Shaikh. 2010. The nutritional and clinical significance of lipid rafts. *Curr. Opin. Clin. Nutr. Metab. Care.* **13:** 156–166.
6. Kim, W., Y-Y. Fan, R. Barhoumi, R. Smith, D. N. McMurray, and R. S. Chapkin. 2008. n-3 polyunsaturated fatty acids suppress the localization and activation of signaling proteins at the immunological synapse in murine CD4+ T cells by affecting lipid raft formation. *J. Immunol.* **181:** 6236–6243.
7. Shaikh, S. R., A. C. Dumaual, A. Castillo, D. LoCascio, R. A. Siddiqui, W. Stillwell, and S. R. Wassall. 2004. Oleic and docosahexaenoic acid differentially phase separate from lipid raft molecules: a comparative NMR, DSC, AFM, and detergent extraction study. *Biophys. J.* **87:** 1752–1766.
8. Soni, S. P., D. S. Locascio, Y. Liu, J. A. Williams, R. Bittman, W. Stillwell, and S. R. Wassall. 2008. Docosahexaenoic acid enhances segregation of lipids between raft and nonraft domains: ^{2}H-NMR study. *Biophys. J.* **95:** 203–214.
9. Grimm, M. O. W., J. Kuchenbecker, S. Grösgen, V. K. Burg, B. Hundsdörfer, T. L. Rothhaar, P. Friess, M. C. de Wilde, L. M. Broersen, B. Penke, et al. 2011. Docosahexaenoic acid reduces amyloid beta production via multiple pleiotropic mechanisms. *J. Biol. Chem.* **286:** 14028–14039.
10. Aliche-Djoudi, F., N. Podechard, M. Chevanne, P. Nourissat, D. Catheline, P. Legrand, M-T. Dimanche-Boitrel, D. Lagadic-Gossmann, and O. Sergent. 2011. Physical and chemical modulation of lipid rafts by a dietary n-3 polyunsaturated fatty acid increases ethanol-induced oxidative stress. *Free Radic. Biol. Med.* **51:** 2018–2030.
11. Bonilla, D. L., L. H. Ly, Y-Y. Fan, R. S. Chapkin, and D. N. McMurray. 2010. Incorporation of a dietary omega 3 fatty acid impairs murine macrophage responses to Mycobacterium tuberculosis. *PLoS ONE.* **5:** e10878.
12. Ruth, M. R., S. D. Proctor, and C. J. Field. 2009. Feeding long-chain n-3 polyunsaturated fatty acids to obese leptin receptor-deficient JCR:LA-cp rats modifies immune function and lipid-raft fatty acid composition. *Br. J. Nutr.* **101:** 1341–1350.
13. Winer, D. A., S. Winer, L. Shen, P. P. Wadia, J. Yantha, G. Paltser, H. Tsui, P. Wu, M. G. Davidson, M. N. Alonso, et al. 2011. B cells promote insulin resistance through modulation of T cells and production of pathogenic IgG antibodies. *Nat. Med.* **17:** 610–617.
14. Hikada, M., and M. Zouali. 2010. Multistoried roles for B lymphocytes in autoimmunity. *Nat. Immunol.* **11:** 1065–1068.
15. Rockett, B. D., A. Franklin, M. Harris, H. Teague, A. Rockett, and S. R. Shaikh. 2011. Membrane raft organization is more sensitive to disruption by (n-3) PUFA than nonraft organization in EL4 and B cells. *J. Nutr.* **141:** 1041–1048.
16. Rockett, B. D., M. Salameh, K. Carraway, K. Morrison, and S. R. Shaikh. 2010. n-3 PUFA improves fatty acid composition, prevents palmitate-induced apoptosis, and differentially modifies B cell cytokine secretion in vitro and ex vivo. *J. Lipid Res.* **51:** 1284–1297.
17. Kim, W., D. N. McMurray, and R. S. Chapkin. 2010. n-3 polyunsaturated fatty acids–physiological relevance of dose. *Prostaglandins Leukot. Essent. Fatty Acids.* **82:** 155–158.
18. Shaikh, S. R., B. D. Rockett, M. Salameh, and K. Carraway. 2009. Docosahexaenoic acid modifies the clustering and size of lipid rafts and the lateral organization and surface expression of MHC class I of EL4 cells. *J. Nutr.* **139:** 1632–1639.
19. Stulnig, T. M., J. Huber, N. Leitinger, E. M. Imre, P. Angelisova, P. Nowotny, and W. Waldhausl. 2001. Polyunsaturated eicosapentaenoic acid displaces proteins from membrane rafts by altering raft lipid composition. *J. Biol. Chem.* **276:** 37335–37340.
20. Davis, J. H., K. R. Jeffrey, M. Bloom, M. I. Valic, and T. P. Higgs. 1976. Quadrupolar echo deuteron magnetic resonance spectroscopy in ordered hydrocarbon chains. *Chem. Phys. Lett.* **42:** 390–394.
21. Bacia, K., D. Scherfeld, N. Kahya, and P. Schwille. 2004. Fluorescence correlation spectroscopy relates rafts in model and native membranes. *Biophys. J.* **87:** 1034–1043.
22. Parasassi, T., G. De Stasio, A. d'Ubaldo, and E. Gratton. 1990. Phase fluctuation in phospholipid membranes revealed by Laurdan fluorescence. *Biophys. J.* **57:** 1179–1186.
23. Miguel, L., D. M. Owen, C. Lim, C. Liebig, J. Evans, A. I. Magee, and E. C. Jury. 2011. Primary human CD4^{+} T cells have diverse levels of membrane lipid order that correlate with their function. *J. Immunol.* **186:** 3505–3516.
24. Rockett, B. D., M. Harris, and S. R. Shaikh. 2012. High dose of an n-3 polyunsaturated fatty acid diet lowers activity of C57BL/6 mice. *Prostaglandins Leukot. Essent. Fatty Acids.* In press. doi.org/10.1016/j.plefa.2011.12.001.
25. Zech, T., C. S. Ejsing, K. Gaus, B. de Wet, A. Shevchenko, K. Simons, and T. Harder. 2009. Accumulation of raft lipids in T-cell plasma membrane domains engaged in TCR signalling. *EMBO J.* **28:** 466–476.
26. Switzer, K. C., Y-Y. Fan, N. Wang, D. N. McMurray, and R. S. Chapkin. 2004. Dietary n-3 polyunsaturated fatty acids promote activation-induced cell death in Th1-polarization murine CD4^{+} T-cells. *J. Lipid Res.* **45:** 1482–1492.
27. Shaikh, S. R., V. Cherezov, M. Caffrey, S. P. Soni, D. LoCascio, W. Stillwell, and S. R. Wassall. 2006. Molecular organization of cholesterol in unsaturated phosphatidylethanolamines: X-ray diffraction and solid state ^{2}H NMR reveal differences with phosphatidylcholines. *J. Am. Chem. Soc.* **128:** 5375–5383.
28. Heerklotz, H. 2002. Triton promotes domain formation in lipid raft mixtures. *Biophys. J.* **83:** 2693–2701.
29. Lingwood, D., and K. Simons. 2007. Detergent resistance as a tool in membrane research. *Nat. Protoc.* **2:** 2159–2165.
30. Jin, L., A. C. Millard, J. P. Wuskell, X. Dong, D. Wu, H. A. Clark, and L. M. Loew. 2006. Characterization and application of a new optical probe for membrane lipid domains. *Biophys. J.* **90:** 2563–2575.

31. Stillwell, W., and S. R. Wassall. 2003. Docosahexaenoic acid: membrane properties of a unique fatty acid. *Chem. Phys. Lipids.* **126:** 1–27.
32. Schley, P. D., D. N. Brindley, and C. J. Field. 2007. (n-3) PUFA alter raft lipid composition and decrease epidermal growth factor receptor levels in lipid rafts of human breast cancer cells. *J. Nutr.* **137:** 548–553.
33. Fan, Y-Y., L. H. Ly, R. Barhoumi, D. N. McMurray, and R. S. Chapkin. 2004. Dietary docosahexaenoic acid suppresses T cell protein kinase Cθ lipid raft recruitment and IL-2 production. *J. Immunol.* **173:** 6151–6160.
34. Fan, Y-Y., D. N. McMurray, L. H. Ly, and R. S. Chapkin. 2003. Dietary (n-3) polyunsaturated fatty acids remodel mouse T-cell lipid rafts. *J. Nutr.* **133:** 1913–1920.
35. Mihailescu, M., O. Soubias, D. Worcester, S. H. White, and K. Gawrisch. 2011. Structure and dynamics of cholesterol-containing polyunsaturated lipid membranes studied by neutron diffraction and NMR. *J. Membr. Biol.* **239:** 63–71.
36. Macdonald, J. L., and L. J. Pike. 2005. A simplified method for the preparation of detergent-free lipid rafts. *J. Lipid Res.* **46:** 1061–1067.
37. Kheirallah, S., P. Caron, E. Gross, A. Quillet-Mary, J. Bertrand-Michel, J-J. Fournié, G. Laurent, and C. Bezombes. 2010. Rituximab inhibits B-cell receptor signaling. *Blood.* **115:** 985–994.
38. Lingwood, D., J. Ries, P. Schwille, and K. Simons. 2008. Plasma membranes are poised for activation of raft phase coalescence at physiological temperature. *Proc. Natl. Acad. Sci. USA.* **105:** 10005–10010.
39. van Zanten, T. S., J. Gómez, C. Manzo, A. Cambi, J. Buceta, R. Reigada, and M. F. Garcia-Parajo. 2010. Direct mapping of nanoscale compositional connectivity on intact cell membranes. *Proc. Natl. Acad. Sci. USA.* **107:** 15437–15442.
40. Hsu, C-S., W-C. Chiu, C-L. Yeh, Y-C. Hou, S-Y. Chou, and S-L. Yeh. 2006. Dietary fish oil enhances adhesion molecule and interleukin-6 expression in mice with polymicrobial sepsis. *Br. J. Nutr.* **96:** 854–860.
41. Blok, W. L., M. F. de Bruijn, P. J. Leenen, W. M. Eling, N. van Rooijen, E. R. Stanley, W. A. Buurman, and J. W. van der Meer. 1996. Dietary n-3 fatty acids increase spleen size and postendotoxin circulating TNF in mice; role of macrophages, macrophage precursors, and colony-stimulating factor-1. *J. Immunol.* **157:** 5569–5573.
42. Petursdottir, D. H., and I. Hardardottir. 2007. Dietary fish oil increases the number of splenic macrophages secreting TNF-alpha and IL-10 but decreases the secretion of these cytokines by splenic T cells from mice. *J. Nutr.* **137:** 665–670.
43. Weldon, S. M., A. C. Mullen, C. E. Loscher, L. A. Hurley, and H. M. Roche. 2007. Docosahexaenoic acid induces an anti-inflammatory profile in lipopolysaccharide-stimulated human THP-1 macrophages more effectively than eicosapentaenoic acid. *J. Nutr. Biochem.* **18:** 250–258.
44. Weatherill, A. R., J. Y. Lee, L. Zhao, D. G. Lemay, H. S. Youn, and D. H. Hwang. 2005. Saturated and polyunsaturated fatty acids reciprocally modulate dendritic cell functions mediated through TLR4. *J. Immunol.* **174:** 5390–5397.
45. Zeyda, M., M. D. Säemann, K. M. Stuhlmeier, D. G. Mascher, P. N. Nowotny, G. J. Zlabinger, W. Waldhäusl, and T. M. Stulnig. 2005. Polyunsaturated fatty acids block dendritic cell activation and function independently of NF-kappa B activation. *J. Biol. Chem.* **280:** 14293–14301.
46. Beli, E., M. Li, C. Cuff, and J. J. Pestka. 2008. Docosahexaenoic acid-enriched fish oil consumption modulates immunoglobulin responses to and clearance of enteric reovirus infection in mice. *J. Nutr.* **138:** 813–819.
47. Weise, C., K. Hilt, M. Milovanovic, D. Ernst, R. Rühl, and M. Worm. 2011. Inhibition of IgE production by docosahexaenoic acid is mediated by direct interference with STAT6 and NFκB pathway in human B cells. *J. Nutr. Biochem.* **22:** 269–275.
48. Lauritzen, L., T. M. R. Kjær, T. Porsgaard, M. B. Fruekilde, H. Mu, and H. Frøkiær. 2011. Maternal intake of fish oil but not of linseed oil reduces the antibody response in neonatal mice. *Lipids.* **46:** 171–178.
49. Selvaraj, R. K., and G. Cherian. 2004. Dietary n-3 fatty acids reduce the delayed hypersensitivity reaction and antibody production more than n-6 fatty acids in broiler birds. *Eur. J. Lipid Sci. Technol.* **106:** 3–10.
50. Shaikh, S. R., and M. Edidin. 2007. Immunosuppressive effects of polyunsaturated fatty acids on antigen presentation by human leukocyte antigen class I molecules. *J. Lipid Res.* **48:** 127–138.
51. Sanderson, P., G. G. MacPherson, C. H. Jenkins, and P. C. Calder. 1997. Dietary fish oil diminishes the antigen presentation activity of rat dendritic cells. *J. Leukoc. Biol.* **62:** 771–777.
52. Chapkin, R. S., J. L. Arrington, T. V. Apanasovich, R. J. Carroll, and D. N. McMurray. 2002. Dietary n-3 PUFA affect TcR-mediated activation of purified murine T cells and accessory cell function in co-cultures. *Clin. Exp. Immunol.* **130:** 12–18.